HOLOGRAPHIC INVESTIGATION OF TRANSPARENT MICROPARTICLES

V.V. Dyomin and S.G. Stepanov

Tomsk State University
Received December 11, 1997

Peculiarities of holographic recording of transparent microparticles are analyzed. A new method for determination of the refractive index of transparent microparticles is suggested. A procedure for accounting for the influence of a cell filled with liquid on holographic images of microparticles contained in the cell is developed.

Interest in optical methods for recording of transparent and semitransparent microparticles is caused mainly by the necessity in investigation of hydrosol microstructure parameters in the problems of ocean optics, limnology, biology, and medicine (study of plankton, physiological hydrosols, and so on). Efficiency of use of the holographic method for solution of these problems was noted in a number of papers.[1,2] The contactless character of such methods allows investigation of vivid microobjects, for example, in a water sample, not perturbing them. Feasibility to determine the microparticle shape using their holographic images is also important, because it allows not only detection, but also identification of particles. For example, it allows one to determine in what type of living organisms are biological microobjects.

Certainly, the problem of investigation of transparent microparticles arises in the aerosol optics as well. However, in most cases, holographic images of transparent and opaque aerosol microparticles are similar. Reference 3 presents the conditions, violation of which leads to the necessity to take into account transparency of microobjects in the process of recording, reconstruction, and interpretation of their images (the condition of far zone and the condition of optical smoothness of a microparticle). It is noted that such necessity can arise when using the holographic scheme with image transfer (including recording of aerosols) and also in case of recording of optically smooth microparticles, i.e. microparticles which refractive index close to refractive index of an ambient medium. The latter situation often takes place when studying microparticles in liquid media.

Known is the feasibility of direct use of holography, without application of special phase-contrast methods, i.e. to visualize phase microobjects (see, for example, Ref. 4). A number of peculiarities of holographic images, such as their contours, uniformity over image field, and so on, seemingly connected with optical properties of recorded microobjects, are observed at holographic recording of transparent and semi-transparent particles. The method for determination of the refractive index of a transparent microparticle from its holographic image is presented in this paper. Experimental tests of this method were performed both for particles being in air and for particles suspended in liquid.

Ensemble of microparticles contained in a sample embedded in cell is the object under investigation in a number of problems. In these cases, the optical system of "liquid−cell walls−air" interface also participates in the process of holography image formation in addition to optical elements of the holography recording system. (The similar situation will occur when using the submersible recording system). The method to take into account the influence of this additional optical system is proposed in the present paper.

DETERMINATION OF REFRACTIVE INDEX OF TRANSPARENT MICROPARTICLES

It is known that two waves: diffracted (*2*) and refracted (*3*) propagate beyond the transparent (or semitransparent) particle (*1*) (Fig. 1*a*). (Radiation re-reflected at microparticle boundaries can be neglected when describing the method, but it seemingly must be taken into account when interpreting holographic images of complex-shaped microparticles.) The refracted wave is focused near the particle and then propagates with far greater divergence than the diffracted wave. Therefore, when recording the hologram *5* in the particle far zone and observing the holographic image through the microscope with a limited aperture, the refracted field *3* can be neglected, and we can assume that an opaque particle is recorded. This simplification is valid for many experiments on aerosol recording.
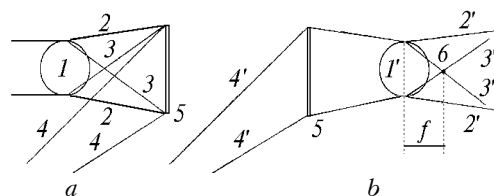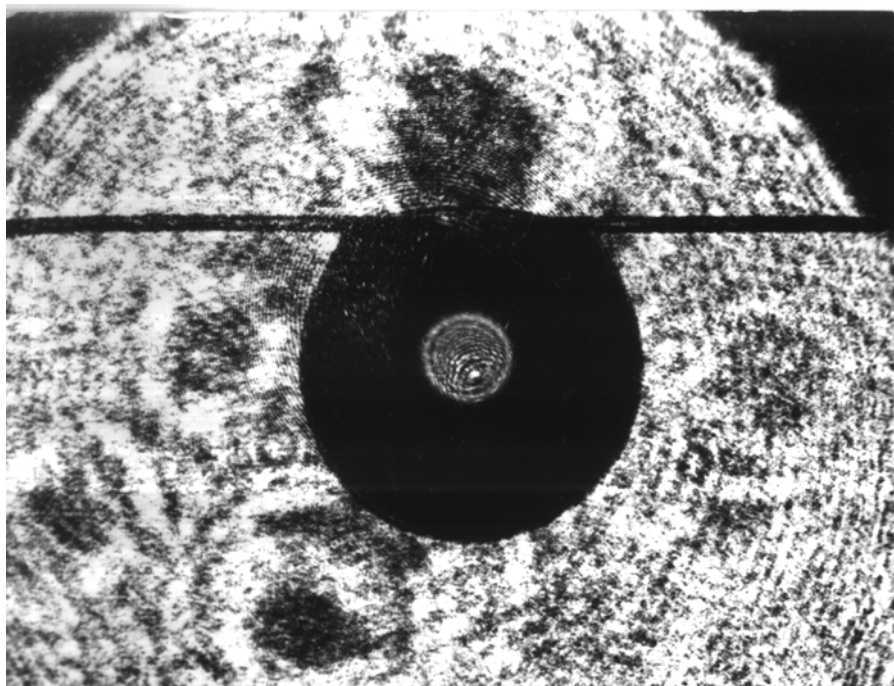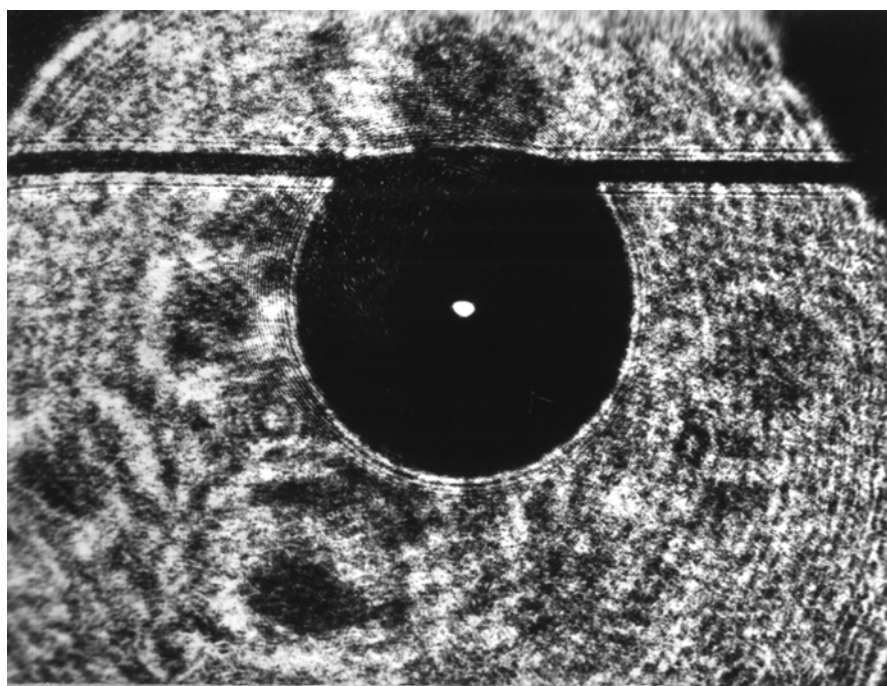

FIG. 1. *Recording (a) and reconstruction (b) of hologram of a transparent spherical particle: microparticle (1), its holographic image (1′), diffracted wave (2, 2′), refracted wave (3, 3′), reference (reconstruction) wave (4, 4′), hologram (5), focusing point of refracted wave (6), focusing distance (f).*

a

b

FIG. 2.   *Pictures of holographic image of an air-borne water droplet: the microscope is focused at the droplet central cross section (a), the microscope is focused at the convergence point of refracted rays (b).*

If the microparticle *1* (or its image in the system of hologram recording with image transfer) is near the plane of hologram *5* recording, the point of refracted radiation focusing *6* will be observed in the reconstructed image in addition to the particle *1'* (Fig. 1*b*). The same effect can be observed for the case of optically smooth particle, when its refractive index is close to the refractive index of an ambient medium.

The distance *f* from the central cross section of the particle with the size *a* to the point of refracted radiation focusing is the function of the refractive indexes of the particle *n* and the ambient medium n_1: $f = f(n, n_1)$. Thus, for a spherical particle this relation can be easily obtained from the experiment geometry. Indeed, if the transparent microparticle is considered as a thick lens, the following expression can be obtained:

$$f = an / [2 (n - n_1)]. \tag{1}$$

This expression is apparently valid for paraxial focus, i.e. rays propagating near optical axis of the system will be focused at this distance.

Then, the refractive index of the particle *n* can be obtained by measuring the distance *f* and the particle radius *a* at the holographic image with known n_1. The error in this case depends mainly on the accuracy of measurement of the refocusing value of the magnifying optical system (for example, the measuring microscope).

The analytic form of the function $f = f(a, n, n_1)$ is, as a rule, quite difficult to be obtained for the case of microparticle with nonspherical shape. Therefore, the numerical methods should be necessarily used for calculation and interpretation of experimental results. One of possible algorithms for calculation is given in Ref. 3.

Experiments for holographic recording of water droplets fixed on a thread verify the efficiency of this method. The off-axis scheme of hologram recording was used in the experiment, droplet radius was 100–200 μm, the continuous He–Ne laser was used as the radiation source. Figure 2 presents the pictures of two cross sections of solid holographic image of a water droplet: the plane of the droplet central cross section and the focusing plane of the refracted wave. The similar experiments were performed with spherical polystyrene particles suspended in glycerin. In both cases, the error of refractive index estimation was 10% and was caused by the measurement accuracy of the microscope refocusing value.

HOLOGRAPHIC RECORDING OF A MICROPARTICLE IN LIQUID

Let us consider the situation shown in Fig. 3. The spherical particle is in the medium with the refractive index n_1, the refractive indexes of the cell walls and the medium outside the cell (the medium where the hologram is located) are n_2 and n_3, respectively. In this case, the object of holography is the particle image located at the point O_1, rather than the particle itself located at the point O (see Fig. 3). Let us reveal the relations between the distances OO_3, O_1O_3, and O_2O_3, because having these relations known and with coordinate of the cell outer wall (O_3) determined from experiment, we can find all the above distances.
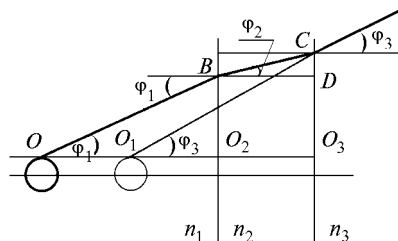

FIG. 3. On calculation of the particle position in the cell.

Toward this aim let us consider the arbitrary ray OB within the diffraction angle φ_1 on the particle edge ($\sin\varphi_1 = \lambda / d$, where λ is wavelength of incident radiation and d is the particle diameter). It should be noted that resolution of the holography is restricted to large particles $\lambda \ll d$, i.e. $\sin\varphi_1 = \mathrm{tg}\varphi_1 \approx \varphi_1$. Considering that in most cases the cell walls are made of glass and air is the medium where the hologram is located, it is easy to verify that the smallness of the angles φ_2 and φ_3 arises from the smallness of the angle φ_1. Then the same condition: $\sin\varphi_2 = \mathrm{tg}\varphi_2 \approx \varphi_2$ and $\sin\varphi_3 = \mathrm{tg}\varphi_3 \approx \varphi_3$ holds true for them, and the Snellius-Cartesian law can be written in the following form:

$$n_1 \, \varphi_1 = n_2 \, \varphi_2 = n_3 \, \varphi_3. \tag{2}$$

From the geometry of Fig. 3 we can write the following relations:

$$CO_3 = O_1O_3 \, \mathrm{tg} \, \varphi_3 = O_1O_3 \cdot \varphi_3,$$

$$CO_3 = CD + DO_3 = BD \cdot \mathrm{tg}\varphi_2 + BO_2 =$$

$$= O_2O_3 \cdot \varphi_2 + OO_2 \cdot \varphi_1$$

or equating the right-hand sides,

$$O_2O_3 \, \varphi_2 + OO_2 \, \varphi_1 = O_1O_3 \, \varphi_3. \tag{3}$$

From Eqs. (2) and (3) we can find the required relations:

$$OO_2 = O_1O_3 \, \frac{n_1}{n_3} - O_2O_3 \, \frac{n_1}{n_2} \, ; \tag{4}$$

$$OO_3 = OO_2 + O_2O_3 = O_1O_3 \, \frac{n_1}{n_3} - O_2O_3 \left(\frac{n_1}{n_2} - 1 \right) \tag{5}$$

and finally

$$OO_1 = OO_3 - O_1O_3 = O_1O_3 \left(\frac{n_1}{n_3} - 1 \right) - O_2O_3 \left(\frac{n_1}{n_2} - 1 \right). \tag{6}$$

Thus, the position of the real particle with respect to the outer wall of the cell (distance OO_3) and the distance between the real and observed particle OO_1 can be determined from experimental measurements of the distance O_1O_3 between the observed image and the outer wall of the cell in the holographic image with known thickness of the cell walls O_2O_3, as well as indexes n_1, n_2, and n_3.

Let us consider now the path of refracted rays interesting for us from the viewpoint of estimation of the particle refractive index n. The similar situation is observed here (Fig. 4), i.e. the point F of the paraxial focus of the refracted rays should be distinguished from its observed image F_1. Let us calculate the relation between the distance OF (equivalent to f in Eq. (1)) and the distance O_1F_1 measured in experiment.
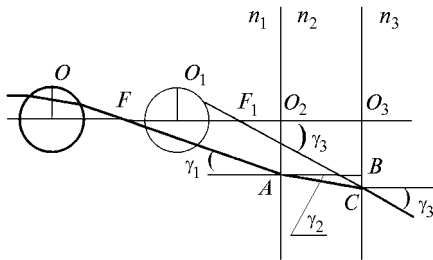

FIG. 4. On calculation of the position of focusing point of rays refracted by the particle in the cell.

It should be noted that we consider the focusing point of rays propagating near the system optical axis. Indeed, spherical particle can be considered as a thick lens with high spherical aberration, therefore for each couple of points on the particle surface located far from the optical axis there exists their own cross point. However, when observing the refracted radiation using a microscope with limited numerical aperture, all rays propagating at large angles will be vignetted by the microlens mount. (The dark ring-shaped zone in the particle image (Fig. 2) is just caused by this fact). Therefore, the condition $\mathrm{tg}\gamma = \sin\gamma = \gamma$ may be thought of as true for the angles γ_1, γ_2, and γ_3, and the Snellius law, as in the above calculation, can be written in the following form:

$$n_1\gamma_1 = n_2\gamma_2 = n_3\gamma_3 . \tag{7}$$

Let us perform the geometrical consideration similar to the above one:

$$O_3C = F_1O_3\, \mathrm{tg}\gamma_3 = F_1O_3 \cdot \gamma_3,$$
$$O_3C = O_3B + BC = O_2A + BC = FO_2\, \mathrm{tg}\gamma_1 +$$
$$+ O_2O_3\, \mathrm{tg}\gamma_2 = FO_2 \cdot \gamma_1 + O_2O_3 \cdot \gamma_2,$$

and consequently

$$F_1O_3 \cdot \gamma_3 = FO_2 \cdot \gamma_1 + O_2O_3 \cdot \gamma_2. \tag{8}$$

Using Eqs. (7) and (8) we obtain

$$FO_2 = F_1O_3\, \frac{n_1}{n_3} - O_2O_3\, \frac{n_1}{n_2} =$$
$$= (O_1O_3 - O_1F_1)\, \frac{n_1}{n_3} - O_2O_3\, \frac{n_1}{n_2} . \tag{9}$$

Having found the distance OF, $OF = OO_3 - FO_2 - O_2O_3$ and using Eqs. (9) and (5), we obtain the final expression

$$OF = O_1F_1\, \frac{n_1}{n_3} . \tag{10}$$

Thus, Eq. (10) describes the relation between the sought distance OF (between the central cross section of the particle and the focusing point of the refracted rays) and the experimentally measured distance O_1F_1.

EXPERIMENTAL RESULTS

Experimental investigations were performed using the spherical polystyrene particles with radius from 200 to 800 μm fixed on the needle point. The feasibility to measure the distances OO_3, OF, O_2O_3, and O_1F_1 (see Figs. 3 and 4) were provided in experiment with the use of the horizontal microscope, when the particle was in air, in the empty glass cell ($n_2 = 1.52$), and also when the same particle (without displacement) was in the cell filled with glycerin ($n_1 = 1.47$). The microscope was referred to the outer wall of the cell. "esides, controlled displacement of the particle in the cell was provided using the micrometric shift.

The measurements were performed in the following order. With air-borne particle fixed on the needle, the coordinates of the points O and F were determined. Then the empty cell was added to the system (in such a way, that the particle was in the cell), and the distances O_1O_3 and O_1F_1 were measured by the sequential focusing of the horizontal microscope at the outer wall of the cell (O_3), at the point F_1 (the observed paraxial focus of refracted rays), and at the image of the central cross section of the particle (O_1) (see Figs. 3 and 4). Then the cell was filled with glycerin and the same measurements were performed. The particle hologram recording was performed in all the considered cases by the off-axis scheme. Then, after the photochemical processing of the hologram, the same distances were measured in the holographic images. Each measurement was performed 10 times with following averaging. In addition, all measurements were done for the cases when the particle was displaced in the cell by a given distances (1, 2, 3, 5, 7, and 11 mm) from the initial position.

TABLE I.

Condition of experiment	Particle displacement, mm	$n\,n_1$, mm	n_1F_1, mm	n
$a = 658$ μm, a particle in an empty cell (direct measurements); $<n_1F_1> = 0.89 \pm 0.04$, $<n> = 1.59 \pm 0.04$ (without a cell $<n\,F> = 0.85 \pm 0.05$, $<n> = 1.63 \pm 0.06$)	1	1.06 ± 0.05	0.89 ± 0.04	1.59 ± 0.05
	2	1.04 ± 0.05	0.90 ± 0.01	1.58 ± 0.01
	3	1.04 ± 0.05	0.87 ± 0.05	1.61 ± 0.06
	4	1.00 ± 0.07	0.93 ± 0.05	1.55 ± 0.04
	6	1.00 ± 0.08	0.90 ± 0.01	1.58 ± 0.01
$a = 658$ μm, a particle in a cell with glycerin (direct measurements); $<n_1F_1> = 3.82 \pm 0.07$, $<n> = 1.61 \pm 0.01$ (without a cell $<n\,F> = 0.85 \pm 0.05$, $<n> = 1.63 \pm 0.06$)	1	2.13 ± 0.05	3.82 ± 0.16	1.61 ± 0.01
	2	2.40 ± 0.02	3.70 ± 0.08	1.61 ± 0.01
	3	2.78 ± 0.02	3.85 ± 0.06	1.61 ± 0.01
	4	3.08 ± 0.04	3.75 ± 0.08	1.61 ± 0.01
	5	3.42 ± 0.07	3.89 ± 0.08	1.61 ± 0.01
	6	3.75 ± 0.05	3.85 ± 0.11	1.61 ± 0.01
$a = 783$ μm, a particle in a cell with glycerin (measurement from a hologram); $<n_1F_1> = 5.22 \pm 0.14$, $<n> = 1.59 \pm 0.01$ (without a cell $<n\,F> = 1.00 \pm 0.02$, $<n> = 1.64 \pm 0.02$)	0	0.88 ± 0.04	5.02 ± 0.16	1.59 ± 0.01
	3	1.76 ± 0.09	5.35 ± 0.13	1.59 ± 0.01
	7	3.00 ± 0.02	5.29 ± 0.02	1.59 ± 0.01
	11	3.66 ± 0.05	5.23 ± 0.17	1.59 ± 0.01
$a = 215$ μm, a particle in a cell with glycerin (measurement from a hologram); $<n_1F_1> = 1.12 \pm 0.12$, $<n> = 1.62 \pm 0.02$ without a cell $<n\,F> = 0.30 \pm 0.02$, $<n> = 1.56 \pm 0.02$)	0	2.74 ± 0.06	1.20 ± 0.12	1.62 ± 0.02
	3	3.78 ± 0.05	1.09 ± 0.08	1.63 ± 0.01
	7	5.66 ± 0.06	1.23 ± 0.08	1.61 ± 0.01

Experimental results were compared to the results calculated by Eqs. (5) and (6), and the particle refractive index n was determined using Eqs. (1) and (10). Some data are shown in the Table I to illustrate these results.

The experimentally obtained data are in good agreement with the calculated one, and their spread allows estimation of the error in determination of the particle refractive index − up to 10%. This error was caused mainly by the accuracy of microscope refocusing (100 μm) and subjectivity of the microscope adjustment for sharpness. It is especially marked with smaller particle size (see, for example, the data for the particle with size of 215 μm). On this basis, the measurement accuracy can be increased by using the precision measuring microscope and computerizing the image processing.

CONCLUSION

The performed measurements have shown that the refractive index of disperse-medium particles can be determined from the hologram. The error of experimental data (10%) can be decreased by increasing the accuracy of the measuring microscope and computerizing the measurement process.

The method for taking into account the influence of the optical system of the "liquid − cell walls − air" interface is proposed and experimentally tested. The method increases the accuracy of estimation of the particle refractive index for the case when liquid disperse medium in the cell is the object of holography processing.

Thus, it is shown that holographic methods allow determination of not only geometrical, but also optical parameters of particles in disperse media.

REFERENCES

1. V.V. Dyomin and V.V. Sokolov, SPIE Proceedings **2678**, 534−542 (1996).
2. V.V. Dyomin, SPIE Proceedings **2678**, 543−547 (1996).
3. V.V. Dyomin and V.V. Sokolov, Atmos. Oceanic Optics **8**, No. 8, 641−645 (1995).
4. S.L. Cartwright, P. Dunn, and ".J. Thompson, Optical Engineering **19**, No. 5, 727−733 (1980).